A Proposed VHF Observing System for the VLA/EVLA: Technical and Management Description

L. J. Greenhill, R. Blundell
(Harvard-Smithsonian CfA),
C. L. Carilli, R. A. Perley
(NRAO)

1. Summary

The key science goal of the proposed program (AG686–see Appendices A, B) is detection of HI emission from the cosmological epoch of reionization. The magnitude of the signal predicted by cosmological models is on the order of 10 to 100 mK. Our initial list of three targets requires an observing band of $\sim$ 186-202 MHz, to obtain spectral channels on and off-line over a 12.5 MHz band.

To detect the predicted line emission, we propose to position crossed dipole antennas below the sub-reflector of each VLA/EVLA antenna, in an arrangement similar to what is used for the existing 74 MHz and 320 MHz observing systems. In our preferred deployment plan, the dipole assemblies will be clamped to the 320 MHz dipole assemblies, and the VHF receivers will be placed in the barrel cabins behind the sub-reflectors. IF signal processing and correlation for VHF band data is not expected to require additional modifications to VLA/EVLA systems, apart from selection of filters and LO frequencies that are under control of the existing real-time system. The VHF observing system is being designed for high sensitivity (Stokes I), low operational overhead, and simplicity of installation. Minimizing impact on the performance of the antennas at other wavebands is also a priority. After commissioning, the VHF system will be given to the NRAO for community use.

If the proposed VHF observing system is approved, then the Smithsonian Astrophysical Observatory (SAO) will build and deliver 28 dipole-receiver packages for deployment and testing. Installation on each antenna will require a small investment of manpower by NRAO operations, but SAO engineering and technical staff will be available to assist. Deployment and testing will involve three stages: (1) mounting of one VHF prototype on a VLA/EVLA antenna for assessment of antenna and receiver performance, RFI environment, and impact on system performance for other wavebands; (2) mounting three VHF prototypes for interferometric testing; and (3) deployment of 28 systems, in a final configuration.

We propose to begin testing in the winter of 2005 and, contingent on results, have the full deployment ready for "first science" during the late-2005 D configuration. The timeline is driven by a need to demonstrate operation and to collect useful data in preparation for the 2007 D configuration, for which deep integrations will be proposed. These two D configurations are important because our key science targets will be visible at night, when manmade RFI is lowest and solar interference is not a consideration. The next suitable D

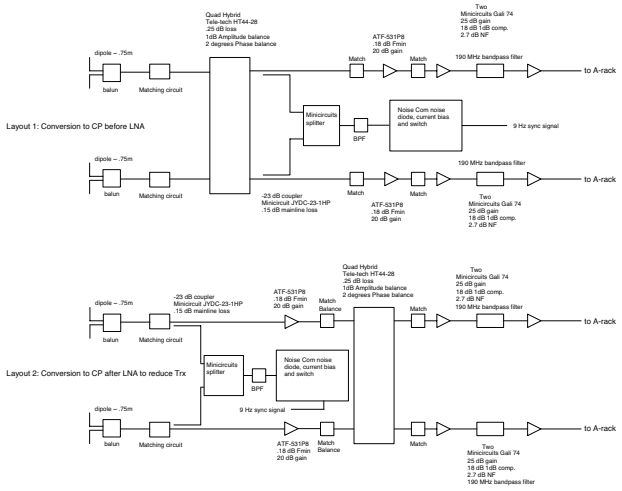

Fig. 1.— Two possible RF layouts of which we will choose one. The feeds are linearly polarized, and receiver outputs are circular. The bottom layout places the quadrature hybrid after the LNA to reduce the system temperature. In this arrangement, LNA gains must be stablized to assure reasonable purity of circular polarization at the output of the hybrid. Each RF module would be insulated and heated above ambient. (Heaters, temperature sensors, DC power supplies, and regulators are not shown.

configuration won't be until 2009.

The proposed VHF observing system will enable a range of "legacy science" by the community, in addition to the key science that is driving system development (Appendix B). We anticipated that frequencies near 190 MHz are probably the lowest for which sensitive imaging is possible with the VLA/EVLA, because of antenna performance and relative levels of receiver and sky noise. In addition, 190 MHz is probably close to the lowest frequency for which conventional calibration techniques are practical on a regular basis. Taken together, these scientific and technical considerations suggest that a VHF observing capability will be an important long-term addition to the VLA/EVLA.

2. Technical Description

2.1. System Layout

The VHF receiving systems comprise crossed dipole antenna assemblies positioned one quarter wavelength ($\lambda/4$) below the centers of the VLA/ELVA subreflectors. The subreflectors act as ground planes, and the position offset defines the illumination of the primary surfaces. Each crossed dipole assembly delivers two linear polarization channels to an RF module for amplification, injection of a broadband switched calibration signal, and conversion to circular polarization via a two sided circuit board design (Figure 1). Two output channels in turn feed the VLA/EVLA antenna A-racks.

The VHF receiver outputs will be com-

bined with the outputs of the 320 and 74 MHz receivers prior to the A-rack, because only one pair of inputs is available. At present, the 320 MHz receiver output for each antenna is combined with the 74 MHz receiver output inside the 74 MHz RF module (at the end of the signal path). Addition of a VHF receiver may be accomplished by extending the "daisy chain," whereby the 74 MHz RF module output is combined with the VHF signal path inside the VHF RF module. The three bands are separable via mixing and filtering in the IF system.

The block design of the VHF RF modules is similar to what is already used at the VLA for the 74 and 320 MHz systems, though with greater attention paid to optimization of noise temperature, as required by the proposed key science. The sky signal will be amplified in three stages without mixing. For purposes of testing, in the initial prototypes conversion to circular polarization will be made after the first amplification stage in an effort to limit system noise. A bandpass-filtered calibration noise source will be coupled to the signal path before the first stage LNA. This noise source will use the same ~ 9 Hz control signal as the 74 and 320 MHz recievers.

2.1.1. Mounting

Two possible mounting schemes for the VHF systems are (1) fixed placement with the dipole assemblies attached to the 320 MHz dipole assemblies (separation ~ 16 cm), and (2) temporary suspension of the dipoles assemblies beneath the subreflectors by rope as is done for the 74 MHz systems (Figures 2, 3). The choice of mount is a significant one as it affects placement of the receiver hardware– see below. Fixed attachment is the preferred choice and will be tried first in field testing. Temporary suspension is considered a fallback.

Fixed Attachment

This is an integrated design approach that entails the lowest operational expense. Each 320 MHz dipole assembly contains two hollow structural support rods that could provide cable paths to the barrel cabin, one for each polarization output of a VHF dipole assembly. Two holes could be drilled in the circular plates that cover the centers of the 320 MHz dipole assemblies. (Seven field units already have the necessary holes drilled–D. Mertely, private communication.) On each antenna, four nonmetallic spacers would be slid over the VHF and 320 MHz dipole arms and held in place with set screws to provide the fixed attachment (Figure 2), and the alignment mirror now attached to the 320 MHz assembly could be moved to the VHF assembly. The RF module would be placed in the barrel cabin, and two coax cables would conduct the amplified VHF signal down the quadrupod, using existing cables, to the A-rack in the Cassegrain cabin. Power for the RF module would be drawn from the existing the 110 VAC supply in the barrel.

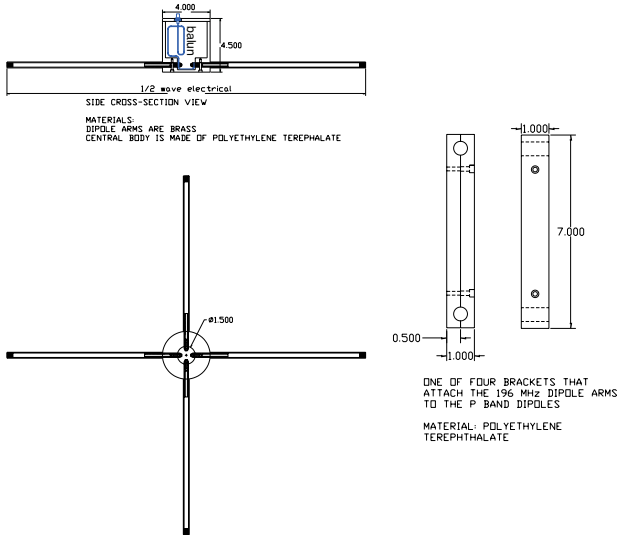

Fig. 2.— Layout for a dipole assembly to be attached to an existing 320 MHz assembly via spacer blocks that slide over the dipole arms and are held in place be set screws (right). The separation is ~ 16 cm. This is the preferred deployment option, subject to evaluation of field tests.

Rope Suspension

This is conceptually the simplest approach, but it entails the operational expense of hoisting VHF dipole assemblies and the one-time cost of installing and threading mount points on the quadrupod legs. The levels of effort will be the same as what has been required for the 74 MHz systems. Choice of rope suspension affects planned placement of the RF modules–they cannot be located in the barrel because it would be too time consuming to connect the coax to/from the dipole assemblies each time they are hoisted. In addition, they cannot be placed in the Cassegrain cabin because a long cable run between from the dipoles (on the order of 8 m) would adversely affect receiver noise temperature. Instead, RF modules would be packaged inside the central hubs of a dipole assemblies (Figure 3). The output signals would be transmitted to the A-racks via pairs of dangling coax cables and existing passthru connectors in the Cassegrain cabin walls. Two additional cables would be needed on each antenna for DC power and control of the calibration noise sources. (DC power would be obtained from the 110 VAC supply in the Cassegrain cabins as part of the SAO installation, with additional regulation in the dipole assemblies.)

2.1.2. Interaction Between VHF and 320 MHz Feeds

Because the VHF and 320 MHz dipole assemblies are close together and optimized for relatively similar frequencies, interaction that might degrade sensitivity in either waveband is a concern. Characterization of losses is critical to selection of how the VHF dipoles will be mounted, and it is best done through

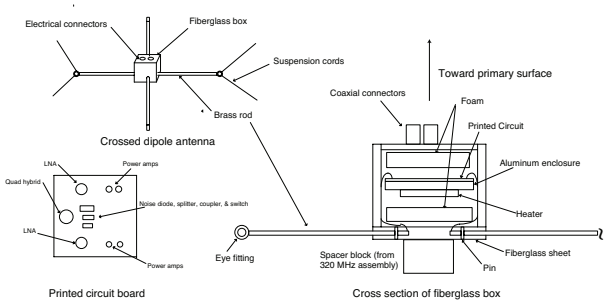

Fig. 3.— Layout for a dipole assembly to be hung by rope beneath a sub-reflector in a style similar to that used for the 74 MHz system. This is a contingency deployment option that would be adopted if, for instance, field testing shows the addition of VHF dipole assemblies significantly degrade system performance for other wavebands.

field testing. However, preliminary loss estimates obtained in lab tests are encouraging, $\ll 1$ dB ($\ll 20\%$ in noise temperature). These tests involved transmission of CW signals (300-350 MHz) and reception by an actual VLA/EVLA dipole assembly and ground plane, with and without a VHF dipole placed in front. (Both elements were $\lambda/4$ from the ground plane, and a load was placed across the VHF dipole.) Losses ranged from 0.3 to 0.7 dB at 350 to 300 MHz, respectively (Figure 4). The difference in the on-axis response of a VHF dipole (180-202 MHz) with and without a 320 MHz dipole positioned between it and the ground plane were too small to measure in the lab with certainty.

We note that losses at 320 MHz caused by the VHF dipole may be reduced if the latter is shorted or left open. Additional lab testing will be used to quantify the anticipated improvement in 01/2005. If losses measured during field testing are deemed too great by NRAO, then a switch can be placed inside the dipole assembly at the cost of an added control line./

Comparison of Mounting Schemes

Strengths of fixed attachment include:

- one-time ops cost to mount dipoles;
- receivers sheltered in barrel cabins;
- no dangling/exposed cables in dishes;
- powered elements not visible to other receiver systems.

Weaknesses of fixed attachment include:

- servicing of RF components is difficult;
- practical only if system noise of other receivers are not degraded substantially.

Strengths of the rope suspension are:

- similarity to existing 74 MHz system;
- no long-term impact on other receivers;
- ready servicing of RF components.

Weaknesses of the rope suspension are:

- overhead for hoisting dipole assemblies;
- RF module/cables exposed to weather;
- powered elements suspended in dishes;
- weather and care taken in hoisting impact dipole position and sensitivity;
- susceptible to feedback and saturation.

2.2. Performance

The intrinsic sensitivity of the proposed VHF system is anticipated to be about as good as that of the 320 MHz system, though the VHF system will be several times more efficient for wide field imaging and in the long run may be the preferred low-frequency system for a number of science programs (Appendix B). Table 1 summarizes characteristics and intrinsic performace parameters for the VHF and existing long wavelength systems. The most important considerations are sky temperature, which is comparable to receiver temperature, and aperture efficiency. Extrinsic factors such as RFI and the effects on image dynamic range of extended, polarized galactic foreground emission may also be important.

2.2.1. Noise Temperature

The contribution of the sky background to system temperature is

$$T_{sky} \sim 100(\frac{\nu}{200\mathrm{MHz}})^{-2.75}\ \mathrm{K}$$

in the colder regions of the sky (i.e., away from the galactic plane). At 74 MHz, the sky dominates the system noise, with typical values of order 10^3K. At 320 MHz receiver noise dominates. VHF frequencies near 190 MHz are close to the cross-over point, where the system and sky contributions are comparable, 50 to 100 K each (Table 1).

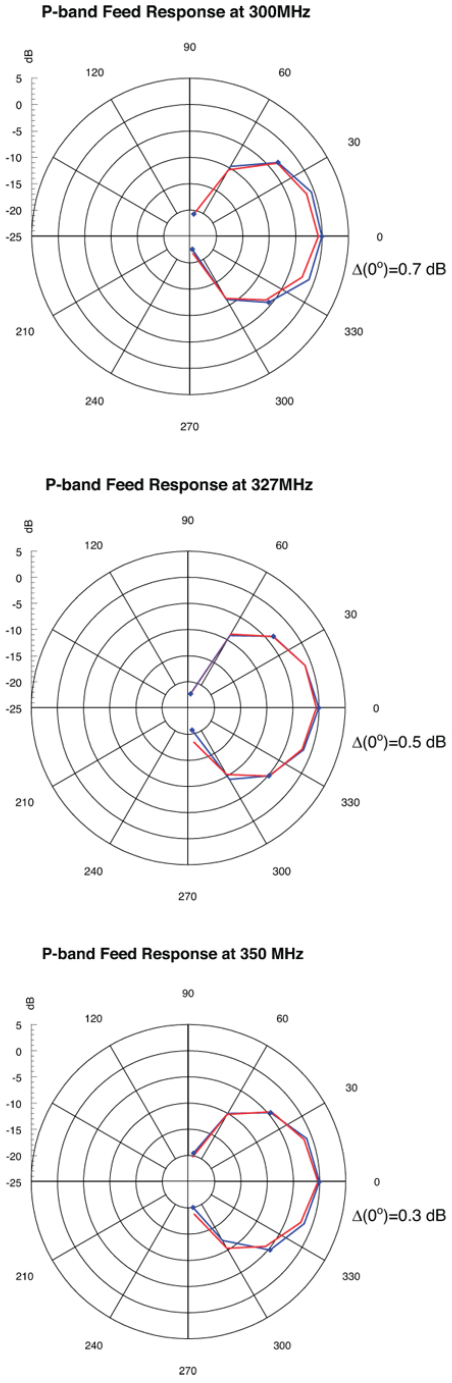

Fig. 4.— Response pattern for a VLA/EVLA 320 MHz dipole assembly (one polarization) with and without a VHF dipole placed in front (red and blue traces, respectively). The dipoles are $\lambda/4$ from the ground plane.

2.2.2. Bandwidth

The performance of the VHF observing system will be optimized for the 12.5 MHz correlator bandwidth (186-202 MHz) needed to observe the initial key science targets. For the mix of components used in the prototype systems, reception over a broader range, 178-208 MHz, will be possible, though with increased system noise. (Lab and field testing will be required to quantify the degradation.) Broaderband components may be available in bulk, which would enable a broader bandwidth for the 28 production dipole-receiver systems, thus benefitting secondary science applications. However, planned use of simple dipoles ($\frac{\Delta\nu}{\nu} \sim 5\%$), a passive balun, and simple matching circuits will probably still limit sensitivity away from 194 MHz.

2.2.3. Aperture Efficiency

VHF frequencies near 190 MHz are close to a "sweet spot." There are two competing phenomena that most strongly affect the efficiencies of VLA/EVLA antennas at low frequency, imperfect focus and diffraction. First, the location of the prime focus is 0.5 m behind the surface of the subreflector (at full retraction), which is the effective phase center for the dipole assemblies. As a fraction of wavlength, losses due to defocusing rise with increasing frequency (Table 1). For a focus error of Δ, the fractional loss according to Ruze (1969) is

$$G/G_o = 1 - [0.42 \times (2\pi\frac{\Delta}{\lambda})^2/(3(4\frac{f}{D})^4)]$$

where $\frac{f}{D} = 0.36$ for the VLA and 0.42 is a numerical constant dictated by the illumination pattern of the primary surface. At 74 MHz, the loss is insignificant, but it increases quadratically with decreasing wavelength. All other factors being equal, if we scale the published aperture efficiency of a VLA antenna at 320 MHz to 194 MHz, then we anticipate an efficiency of $\sim 55\%$.

Working in the opposite sense to the focus loss is the effect of diffraction. The primary surface spans 6, 16, and 27 wavelengths at 74, 194, and 320 MHz, respectively. While defocusing is not a problem at 74 MHz, the system is limited by diffraction, which leads to low efficiency and poor beam shape. At 320 MHz the effects of diffraction are substantially reduced but loss due to poor focus is significant. The calculation of diffractive effects accounting for details of the antenna structure is difficult without a full electromagnetic model. However, we anticipate losses on the order of 10%, and consequently, the balance of losses due to focus and diffraction will probably lead to a relatively high efficiency in the VHF band. (Nonetheless, we note that the best measure of efficiency will come from field testing a prototype VHF receiver on a VLA/EVLA antenna.)

Table 1: VLA Low Frequency Systems

Band [MHz]	Passband [MHz]	A_e	T_{rx} [K]	T_{sky} [K]	D/λ	RMS(10min)* [mJy]	Δ/λ	Focus loss	FoV† [°]	(FoV/scaled rms)^{2}§ [$(^\circ)^2$ mJy^{-2}]
74	73-74.5	0.15	···	10^3	6	150	0.10	0.01	11	0.0054
VHF‡	178-202	0.5	60¶	100	16	0.9	0.27	0.08	4.1	3
320	305-337	0.4	100¶	25	27	1.4	0.43	0.24	2.5	0.17
1400	1240-1700	0.55	30	3	125	0.056	···	···	0.50	0.22

*Assumes bandwidths of 0.781 MHz, 3.125 MHz, 12.5 MHz, and 100 MHz in each polarization at 74 MHz, 194 MHz, 320 MHz, and 1400 MHz, respectively.

†Field of view, half power full width.

§RMS scaled by a presumed source spectral index of -1, referred to 74 MHz.

‡VHF efficiency and noise temperature are best estimates based on initial modeling (NEC4) by W. Brisken. We plan to verify these numbers through testing of scaled models and prototype testing at the VLA.

¶Not including the effects of spillover, probably ~ 20 K based on experience of observers at the GMRT.

2.2.4. Beam Characteristics

The beam pattern of a VLA/EVLA antenna outfitted with a VHF receiver is difficult to anticipate in advance of field testing. Structural details of the antennas can strongly influence the pattern (e.g., curvature and asymmetry of the sub-reflector ground plane). Of particular concern are several characteristics identified in work with the 320 MHz observing system: polarization dependence, angular offsets, squint, and scaling with frequency.

3. RFI

Monitoring of the VHF band at the VLA site has been ongoing since the beginning of 2004 August (Figure 5); see also http://www.vla.nrao.edu/astro/rfi/almamon/plots/lband/). Sources of RFI that are a concern include television broadcasting (Table 2), the VLA clock distribution system, and an episodic source of broadband emission that we hope to identify in winter 2005. One candidate is White Sands (Ridgeway, priv. comm.).

Table 2: Potential Sources of RFI

Source	Frequency* [MHz]	License
Ch 7 audio	179.75	KOAT Albuquerque
		KVIA El Paso
Ch 8 video	181.25	KOBR Roswell
Ch 8 audio	185.75	···
Ch 9 video	187.25	KTSM El Paso
Ch 9 audio	191.75	···
Ch 10 video	193.25	KBIM Roswell
Ch 10 audio	197.75	···
Ch 11 video	199.25	KCHF Santa Fe
Ch 11 audio	203.75	···
Ch 12 video	205.25	KOBF Farmington
White Sands	···	···

*Video channels are 5 MHz wide; audio channels are 1 MHz wide.

At the sensitivity level of the monitoring system, night time observing appears to be practical. Broadband RFI is less common at that time, and TV carriers are weaker. During 2004 August and September half of all days exhibited clear conditions ~ 8 hours per

night. We have requested continued monitoring during the months when our key science targets are visible principally at night (i.e., through May 2005).

Despite the apparently good conditions, the difference in sensitivity to RFI between the monitor system and a VHF receiver mounted on a VLA/EVLA antenna may be very great. The only way to ascertain the actual impact of RFI and to assess mitigation strategies (e.g., notch filters, excision, dynamic scheduling) will be through field testing with prototype receivers. This is one reason that rapid deployment of a prototype receiver has been proposed (see next section and Appendix A).

4. Management Description

4.1. Project Structure

The VHF development program has been proposed and is led by Greenhill and Blundell at the SAO, in collaboration with R. Perley and C. Carilli at the NRAO. A. Loeb and M. Zaldarriaga (Harvard) are also scientific collaborators on the project (Table 3), with involvement of L. Hernquist and B. Gaensler a possibility. The SAO lab spaces, the technical and engineering staff, and investigators Greenhill and Blundell are colocated in one building in Cambridge.

Funding for design and manufacture of all necessary VHF receiver systems has been obtained within the SAO. Funds are also available for travel by SAO engineering and technical staff to the VLA site to support testing and deployment activities. Those activities will be led by Perley and Carilli, but installation of the VHF systems on each antenna will require investment of manpower by NRAO operations in part because access to engineering spaces will be required (e.g., the barrel and cassegrain cabins). Perley and Carilli will be responsible for coordination with SAO staff (on site and in Cambridge) and with NRAO operations so that work does not interfere with VLA operations and EVLA activities.

4.2. Critical Path

The critical path for the proposed VHF project in 2005 comprises testing and deployment milestones. Because the design of the VHF systems is relatively simple there is no intrinsic R&D risk. On the other hand, there are challenges: achieving high antenna efficiency and low system noise, demonstration that the RFI environment is manageable, and demonstration that high dynamic range images can be obtained with or without a full polarization calibration. The field testing program led by Perley and Carilli and synthesis simulations conducted at SAO will settle these issues by 04/15/05.

Milestones in 2004 and 2005 follow.

- 10/01/04: (met)
  Secure SAO funding;
  Proposal to NRAO for $50^h \times 3$ sources
- 11/15/04: (met)

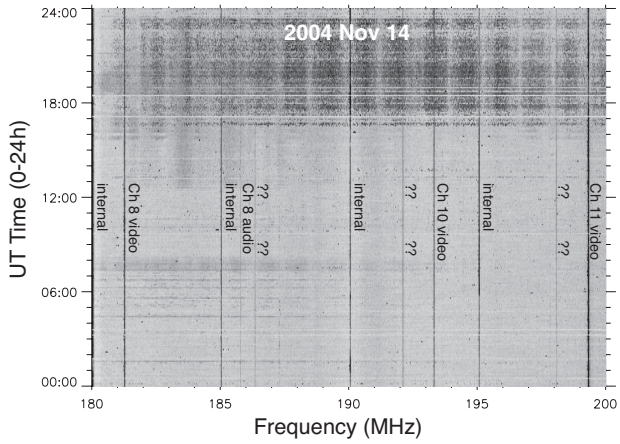

Fig. 5.— Sample RFI plot for the VLA site, with 10 kHz resoluton bandwidth and 5 min time resolution. Clear windows are light gray. Over 48 monitoring days in 2004 August and September, 29 days showed good conditions for > 6 hours and 22 days showed good conditions for ~ 12 hours.

Visit by SAO technical staff to VLA

- 12/10/04: (met)
  Lab measurements to quantify interaction between VHF and 320 MHz dipoles
- 12/23/04: (met)
  Prototype dipole/receiver design
- 02/01/05:
  Deliver first prototype to NRAO
- 02/08/05:
  Install first prototype on a VLA/EVLA antenna for testing
- 02/22/05:
  1^{st} report on antenna/rx performance
  Determine whether RFI is manageable
  Determine impact on other wavebands
  Go/no-Go decision
- 03/08/05:
  Deliver three additional prototypes
  2^{nd} report on antenna/rx performance
- 03/15/05:
  Install new prototypes (4-element array)
  Begin receiver-dipole design review
- 04/15/05:
  Report on inteferometer performance
  Complete reciever-dipole design review
  Begin full production of dipole assemblies and receivers (seven per month)
- 06/01/05:
  "Large" proposal to NRAO for $> 300^h$
- 10/27/05:
  Complete installation of receivers on 28 antennas prior to D configuration

The timing of testing tasks along the critical path is planned largely to avoid dates when NRAO operations will be allocating manpower to array reconfiguration during 01/10-21/05 and 02/14-18/05.

Table 3: Personnel & Responsibilties

Personnel	Inst.	Background(*)	Responsibility
L. Greenhill	SAO	sci	project scientist and manager; data analysis
R. Blundell	SAO	sci/eng	lead for SAO submm receiver lab activities
E. Tong	SAO	eng	system and concept design: antennas and electronics
R. Kimberk	SAO	eng	technical design, construction, and lab testing; deployment
S. Leiker	SAO	eng	technical design, construction, and lab testing; deployment
R. Perley	NRAO	sci/eng	Prototype testing; commissioning; calibration and measurement; data analysis
C. Carilli	NRAO	sci	Prototype testing; commissioning; calibration and measurement; data analysis
A. Loeb	Harvard	sci	Theory and modelling
M. Zaldarriaga	Harvard	sci	Theory and modelling
S. Furlanetto	CalTech	sci	Theory and modelling

*sci: science; eng: engineering; tech: technical

SAO biographies: *L. Greenhill*–SAO radio astronomer (1992-) with experience working on 70/100 m-class apertures, cm-wave interferometers (VLA, Australian LBA, VLBA), and mm/submm-wave interferometers; SAO PI for the proposed MWA meter-wave array. *R. Blundell*–IRAM group head (1980-89) for low noise millimeter heterodyne receiver development; director of the SAO submillimeter receiver laboratory (1989-), supervising receiver and antenna development for the SAO Submillimeter Array; PI for the first ground-based THz observing system. *E. Tong*–CRL-Tokyo (1989-1991) and SAO receiver lab staffmember (1991-) responsible for development of low noise mm/submm heterodyne receivers; near field beam measurement at submm wavelengths. *R. Kimberk*–Harvard College Observatory lead engineer for the MicroObservatory project with experience in optical, mechanical, electronic, and camera design; SAO receiver lab staffmember working principally on antenna servos, LO generation, and LO control electronics. *S. Leiker*–SAO receiver lab staffmember with most recent responsibilities including CAD, cabin temperature control, and optical guidescopes.

4.3. Timeline

The proposed program is divided into four phases.

- *Prototype design and construction (through 02/01/05)* –
  Phase 1 is dedicated to design and construction of a single prototype receiver and dipole assembly, with construction of scale models for lab testing as required. Delivery will be made by 02/01/05. The prototype will be configured for attachment to the 320 MHz dipole assembly because this is the preferred long-term deployment option, and lab test results have suggested interaction between dipole assemblies will probably not be a problem. (However, a contingency design for rope suspension of the VHF dipole assembly is available if required.)

  Phase-1 work will be supervised by Greenhill and Blundell, with assistance from Perley and Carilli in the assessment and characterization of existing VLA/EVLA systems and interfaces. Design, assembly, and test and measurement are being conducted by Tong, Kimberk, and Leiker.

- *Single dish testing at the VLA (02/08 - 03/08/05)* –
  Phase 2 activities will deliver the initial field test results necesssary to make a go/no-go decision in consultation with NRAO management (by 02/22/05), based on (1) key science requirements, (2) antenna and receiver performance, (3) RFI intensity and feasibility of mitigation, and (4) formulation of a practical operational model for a fully deployed VHF system. The test results will also contribute to a design review of the receiver and dipole assembly that begins in phase 3.

  Testing will be directed primarily to assessment of receiver stability, antenna efficiency, system noise as a function of frequency, spillover, beam pattern and centration, RFI as a function of frequency and time, impact on system noise in other wavebands, IF power levels and signal separation (for the 74 MHz, VHF, and 320 MHz bands), dipole mounting schemes, and operational costs. The time required for single antenna testing is difficult to estimate in advance. In one case, it might be accomplished in $\sim$ 1 month, with time available on weekly maintenance days and $\sim$ 1 hour intervals used to characterize nighttime RFI and system noise. If additional time is needed, the VHF-equipped antenna could be removed from the array at times when EVLA activities do not also demand withdrawl of antennas from the array.

  The phase-2 program will be led by Perley and Carilli, with assistance by visiting SAO technical staff (Kimberk or Leiker). Responsibility for analyses of results will be shared among all team members. Construction of the three additional prototype receivers and dipole assmelbies will be completed by Kimberk and Leiker during phase 2, with delivery by 03/08/05.

- *Four element interferometric testing (03/15 - 04/15/05)* –
  Phase 3 will concentrate on assessing (1) the comparative performance of different antennas and (2) the performance of the VHF system in an interferometric mode. Phase 3 will commence with installation of the three additional prototype receivers. Because the array will be in B-configuration ($36''$ beam, comparable to the NVSS beam), the sky will be dominated by relatively compact sources, which will simplify analysis of visibilities. However, it is not yet certain whether receiver polarization "leakage" and the presence of linearly polarized galactic (foreground) emission on angular scales comparable to D configuration fringe spacings will require full Stokes calibration to achieve high dynamic range in science imaging. Through phase 3, this question will be studied via simulations by Greenhill (with the assistance of B. Gaensler and D. Barnes, U. Melbourne) and analysis of data from the VHF subarray. Polarization studies will probably require use of the VHF subarray in

several 8-hour nighttime tracks. Otherwise phase-3 and phase-2 activities will probably be completed in comparable amounts of time.

Phase-3 activities will be led by Perley and Carilli. Greenhill, Blundell, and Tong will lead a parallel design review of the receiver and dipole assembly in preparation for production manufacture.

- *Full production (04/15 - 09/30/05)* – Phase 4 encompasses construction of a full complement of receivers and dipole assemblies, installation on 28 VLA/EVLA antennas, and testing in preparation for science observing. Production of seven units per month is feasible, with delivery beginning in May, 2005. Installation at a rate of seven units per month is preferred, though the proposed schedule would accommodate five per month. Testing for each antenna should require only a few hours during weekly maintenance time.

  Production will be performed by a predoctoral student or research associate in the SAO receiver lab, supervised by Kimberk and Leiker. The requirements for maintenance of SAO technical and engineering staff on site will be determined based experience gained during phases 2 and 3. In principle, installation will be well understood by this point.

We thank Dale Frail for his contribution to the legacy science, Robert Ridgeway for conducting RFI monitoring, and Dan Mertely for valuable discussions of VLA/EVLA hardware. We also thank Walter Brisken for his contributions of technical information, including NEC4 modeling of the VLA antennas at 320 and 194 MHz.

5. References

de Breuck et al. 2002, AJ, 123, 637

Carilli, C., Gnedin, N., & Owen, F. 2002, ApJ, 577, 22

Furlanetto, S. & Loeb, A. 2003, ApJ, 588, 18

Inoue, S. 2004, MNRAS, 348, 999

Ioka, K. 2003 ApJ, 598, L79

Morales, M. & Hewitt, J. 2004, ApJ, 615, 7

Oh, S. P. & Furlanetto, S. R. 2005, ApJ, submitted (astro-ph/0411152)

Palmer, D. M. 1993, ApJ, 417, L25

Perna, R. & Lazzati, D. 2002, ApJ, 580, 261

Rawlings, S. & Jarvis, M.J., 2004, MNRAS, 355, L9

Ruze, J. 1969, MIT Lincoln Lab memo

Sagiv, A. & Waxman, E. 2002, ApJ, 574, 861

Stratta et al. 2004 ApJ, 608, 846

Vreeswijk et al. 2004 A&A, 419, 927

Walmsley, C. M. & Watson, W. D. 1982, ApJ, 260, 317

White, M. et al. 1999, ApJ, 514, 12

Wyithe, A. & Loeb, L. 2004a, Nature, 427, 815

Wyithe, A. & Loeb, L. 2004b, ApJ, 610, 117

Zaldarriaga, M., Furlanetto, S., & Hernquist, L. 2004, ApJ, ApJ, 608, 622

A. Proposal for VLA Observing Time: Program AG686

Proposal AG686 has been nominally accepted for D configuration in 2005, pending technical and management review of plans to outfit the VLA/EVLA with VHF receivers.

A.1. Abstract

We propose to search for HI emission from material surrounding the HII regions of quasars during the cosmological epoch of reionization (EOR). For the three known "EOR quasars" detected by Sloan, the HI line is redshifted to 192-196 MHz. If time is awarded, SAO will build 28 VHF receiving systems, which we will help install in time for commissioning and use in the 2005 and later D-configurations. This VHF system will be open for later community use and operationally similar to the 400 cm system. Little data exist to constrain models of the EOR. With direct imaging, we will constrain the state of the IGM (e.g., warm or cold) and neutral fraction, as well as quasar age, formation time, and ionization anisotropy. The proposed system leverages previous investments in the VLA to accomplish pathfinding EOR science several years before facilities to be built from the ground up for > 10 times the cost.

A.2. Science Justification

The structure and evolution of the universe during the Epoch of Reionization (EOR) are essentially unknown. Analyses of Cosmic Microwave Background (CMB) temperature and polarization fluctuations detected with WMAP have been used to infer reionization began between redshifts 11 and 30 (Kogut et al. 2003, ApJS, 148, 161). Study of Lyα absorption in the optical spectra of quasars indicates a rapid change in the HI neutral fraction of the intergalactic medium (IGM) toward the end of the EOR (Fan et al. 2002, ApJ, 123, 1247), with a substantial neutral fraction as late as $z \sim 6.3$ (Mesinger & Haiman 2004, ApJ, 611, L69). On the other hand, surveys of Lyα selected galaxies at $z \sim 6.6$ have been used to argue for earlier completion of reionization (Hu et al. 2002, ApJ, 568, L75; Malhotra & Rhoads, astro-ph/0407408; Stern et al. astro-ph/0407409), although the interpretation of these results is difficult (e.g., Santos 2004, MNRAS, 349, 1137; Haiman 2002, ApJ, 576, L1). Together these results indicate that the history of reionization probably extended over a large redshift interval and was complex, with multiple peaks (Wyithe & Loeb 2004a, Nature, 427, 815, and references therein).

Characterization of how reionization proceeded may be achieved directly through detec-

tion and interferometric mapping of the HI heated in advance of the ionization fronts that expand relativistically into the IGM during the EOR. Estimation for any redshift of (1) the shape and size of the bubbles on the sky, (2) velocity structure, and (3) amplitude of the signal would provide critical constraints for theory (Wyithe & Loeb 2004b, ApJ, 610, 117). The amplitude is proportional to the neutral fraction (x_{HI}) of the IGM, and the magnitude may be used to estimate whether the IGM is warm ($T_{spin} \gg T_{CMB}$) or cold ($T_{spin} < T_{CMB}$) - Figures 6, 7. In addition, the sizes and shapes of the regions are governed by the ages of the quasars and the anisotropy of ionizing flux emitted by them. From measurement of size it might be possible to constrain how soon after cosmological recombination the first stars and massive dense objects formed.

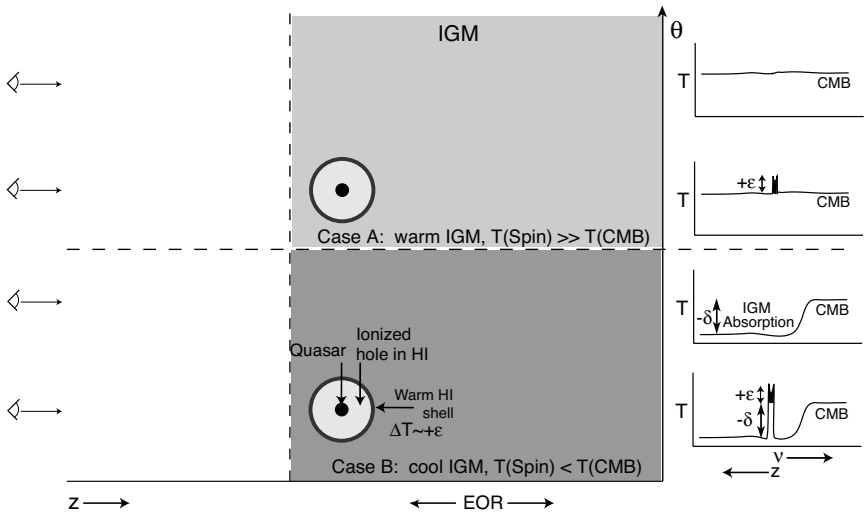

Fig. 6.— HI emission signature of the ionized region around a quasar prior to cosmological reionization. *(bottom)*– Lyα background in the IGM elevates the spin temperature of Hydrogen. If the IGM is largely opaque, then the background is low, and the IGM is cold. In this case $T_{spin} < T_{CMB}$, and HI absorption depresses the CMB (by δ) for frequencies that correspond to $z > 6.2$. However, along lines of sight where a quasar has ionized the HI, the CMB will be unabsorbed. On top of this, there will be emission (ϵ) from a shell of hydrogen surrounding the ionized region and heated by X-rays. The total signal is visible to an interferometer ($\delta + \epsilon$). *(top)*– If $T_{spin} \gg T_{CMB}$, then there is no absorption and only emission from the warm hydrogen is detectable (ϵ).

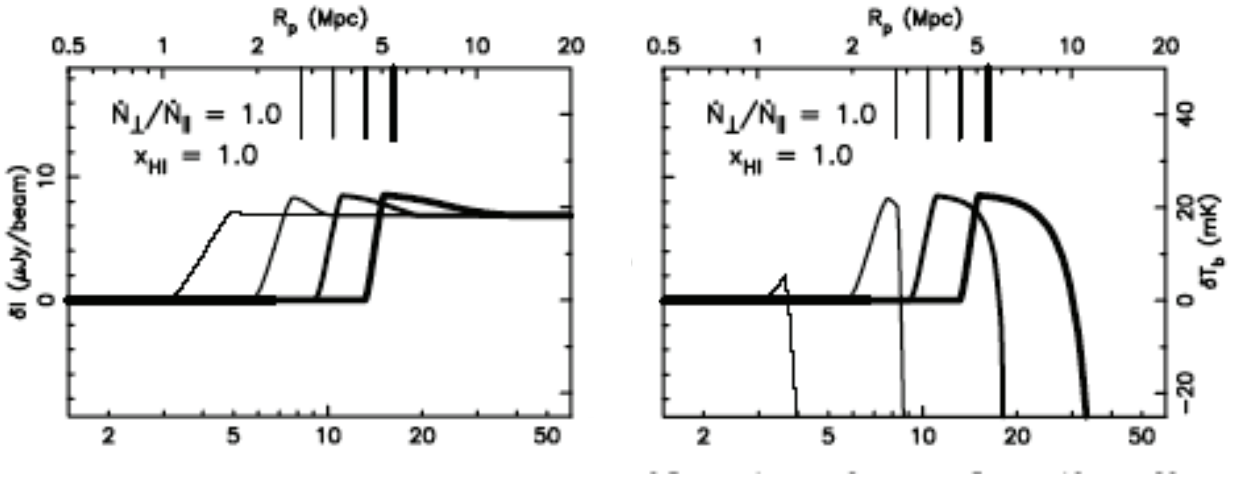

Fig. 7.— Radius of an ionized region in the sky plane and HI line strength, for isotropic quasar emission ($z = 6.5$, $N = 10^{57}$ Ly$\alpha\, s^{-1}$) and a uniform neutral IGM. *(left)*– Warm IGM. *(right)*– Cold IGM, where absorption of the CMB creates a local ~ 320 mK contrast that is detectable by an interferometer. The traces are for quasar ages of (0.5 - 4)$\times 10^7$ yr. The bottom axis is angle on the sky ($'$). From Wyithe & Loeb 2004b.

We propose to directly characterize the IGM and many-Mpc-scale ionized bubbles driven by the three known quasars that "lie in" the EOR (Fan et al. 2001, 2003; AJ, 122, 2833; AJ, 125, 1649): SDSS114816.64 +525150.3 (z = 6.43), SDSS104845.05 +463718.3 (z = 6.23), and SDSS103027.10 +052455.0 (z=6.28).

For these three "EOR quasars," the HI line is redshifted to frequencies of 192-196 MHz and cannot be mapped sensitively with existing low frequency facilities (i.e., GMRT, Westerbork, Molonglo). Innovative new facilities are proposed or under construction, but observing is at least several years away. *We propose to build and contribute to the VLA 28 VHF receiver systems (170-200 MHz) that will enable study of these EOR quasars starting in late 2005 - and higher redshift objects ($z < 7.4$) when they are discovered.* The VHF system will be a pathfinder for EOR science and the new facilities. It will also be a long term addition to the VLA and EVLA, available to the community, and opening a spectral window that is relatively free of RFI (Figure 8). We note the fast pace for construction and deployment is necessary because we may require two D-configurations to complete the project (the first is proposed here), and the targets are up at night in 2005 and 2007, but not 2008. Overall, the accelerated timeline is realistic because the VHF system will be technically and operationally similar to the existing 400 cm system contributed by NRL, i.e., NRL blazed the trail.)

Funding ($\sim$ \$110k) for the design, assembly, and testing of the VHF system has been

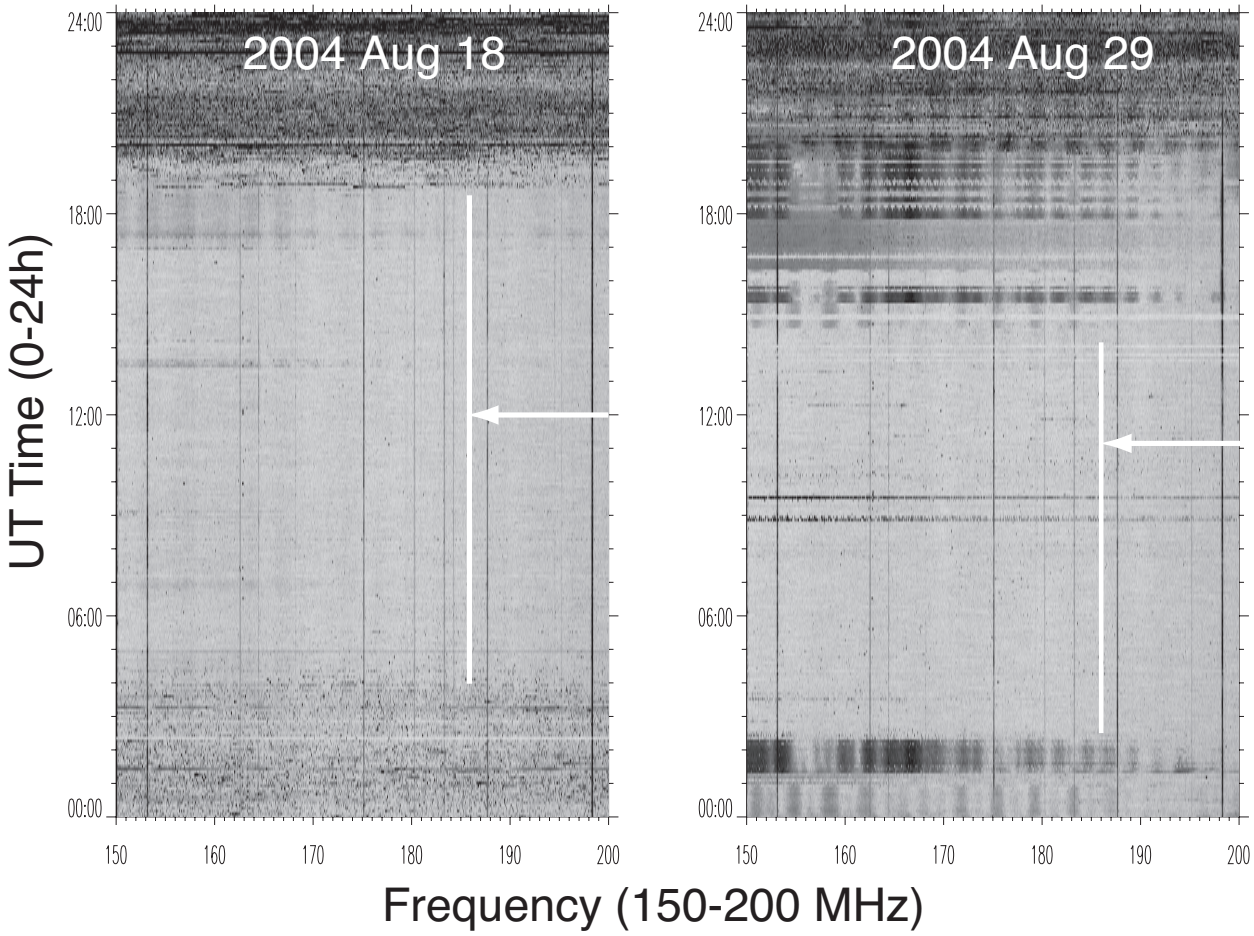

Fig. 8.— Sample RFI plots for the VLA site, with 10 kHz resoluton bandwidth and 5 min time resolution. Vertical white line delimit the proposed observing band. Clear windows are light gray. During mid/late summer 2004, $\sim$ 11 PM to $\sim$ 8 AM is most often clear. Some days are substantially better. Summer lightning causes the black chaff at the top of each plot, and this won't be a factor for the proposed (fall/winter) observing. Narrow vertical black lines are television carriers. Some channels appear to broadcast only carriers most of the time (e.g., 198 MHz). Broad horizotal waves represent modulated transmission, which occurs chiefly during working hours. *Over 48 monitoring days from late 2004 July to late 2004 September, 29 days showed good conditions for* $>$ 6 *hours and 22 days showed good conditions for* $\sim$ 12 *hours.*

secured inside Smithsonian, contingent on the success of this request for observing time. NRAO has indicated that it will consider deploying the VHF system contingent on peer review and delivery of an acceptable technical and management plan. This request for observing time is the next step after approval of funding.

A.3. Technical Justification

The anticipated diameters of the HI emission regions are 10-20′, which is well matched to the tapered beam of the VLA in D-configuration at $\sim$ 194 MHz. (In contrast, the beam of the GBT is too large - and there is no receiver for this band.) Due to cosmological expansion, the line profile is on the order of 2 MHz wide. The best matched VLA correlator mode is 12.5 MHz total bandwidth with 0.8 MHz channel width. In 50 hours, the VLA will achieve $\sim$ 11 mK RMS due to thermal noise, assuming detection of two polarizations, system temperature of 150 K, 26 antennas, 40% aperture efficiency, 78% correlator efficiency, and tapering to achieve a 15′ beam. (In practice, optimal filtering of image data will be used to match the source in frequency and angle, but the listed parameters are reasonable estimates of the results.) To achieve high sensitivity, foreground continuum emission from galactic and extragalactic sources must be eliminated. First, we will subtract strong point sources identified in a *short* integration with an extended configuration (to be proposed later). Second, we will interpolate in frequency and subtract images made off the HI line from images made on the line, incurring a $\sim$ 20% penalty in the RMS. (We have adopted the published VLA efficiency at 320 MHz until we can complete a full electromagnetic analysis at 194 MHz. However, we estimate the 194 MHz system may have similar *or higher* efficiency because it will operate closer to in-focus than the 320 MHz system, $\sim \frac{1}{3}\lambda$ vs $\sim \frac{1}{2}\lambda$ - a difference of $\sim$ 30% in efficiency, which should more than offset at 194 MHz the heightened impact of aperture obstructions. We have also assumed loss of one antenna due to EVLA testing, though loss of three would be acceptable, and we have adopted a preliminary system temperature, based on proximity of the targets to the galactic pole - anticipated $\sim$ 30 K receiver, $\sim$ 20 K spillover as experienced at the GMRT, and $\sim$ 100 K sky temperatures - see Figure 9. The actual system temperature may be on the order of 20% higher due to uncertainties in these quantities.)

Depending on the state of the IGM, the HI signal will be on the order of $23x_{HI}$ mK (warm IGM) or $320x_{HI}$ mK (cold IGM). In an integration of 50 hours, it should be possible to achieve a signal-to-noise ratio (SNR) of 20 to $24fx_{HI}$ for a cold IGM, where f is the beam filling factor of cold material (probably close to unity). It is arguable that toward the end of the EOR a (cold) IGM largely devoid of Lyα background is unlikely. However, we note that there are currently no definitive measurements either way. We propose to use limited integrations on three quasars in 2005 (150 hours) to investigate this "strong signal" case and at the same time conduct extensive hardware and data reduction tests, demonstrating that we can reach predicted noise levels. *In the event the IGM is cold, we will be able to make a statistically significant detection over an almost order of magnitude range in fx_{HI}. Absent a detection, we will establish firmly that the IGM is warmer than the CMB at $z = 6.2$-6.4.*

Investigation of the possilby more likely "weak signal" case will require submission of a large propsoal to NRAO. A 4σ detection could be achieved in ~ 250 hours, for $x_{HI} = 1$ in the vicinity of the quasar. (Since the position of the quasar is known *a priori*, 4σ would be statistically significant.) In addition, we would attempt to detect HI temperature fluctuations due to the evolution of the IGM density and ionization (Zaldarriaga et al. 2004, ApJ, 608, 622) in the 2.5° (very deep) fields around the quasars as a *parallel* experiment. These fluctuations will be too weak to image, but their statistics should be measurable, much as COBE was able to obtain CMB statistics in advance of WMAP imaging. For the D-configuration following 2005, the large proposal deadline is June 1 and precedes commencement of observing. To address this, we will follow submission of a large proposal with monthly updates regarding system performance and initial synthesis results while the proposal is under review, through the end of 2005 or start of 2006.

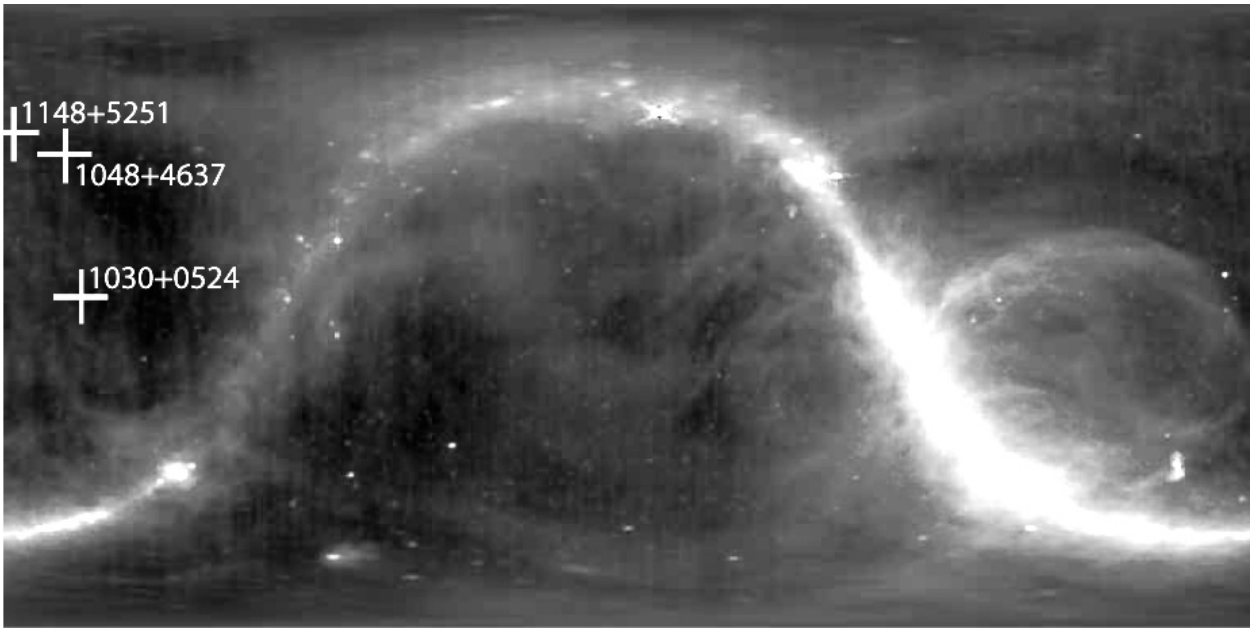

Fig. 9.— All-sky map at 408 MHz (Haslam et al. 1982, A&A, 47, 1; shading by D. Emerson). The proposed targets lie in regions with among the lowest levels of galactic background emission, 14-16K. All lie well away from the galactic plane ($b > 50°$). For 194 MHz, the anticipated sky temperature is $\sim$ 100 K based on global measurements (D. Emerson, www.tuc.nrao.edu/$\tilde{}$demerson/radiosky/rsky_p3.htm; Kraus 1986, Fig. 8-6) or scaling of the Haslam results with frequency ($T_{sky} \propto \nu^{-2.7}$).

B-1. Key and Legacy Science

B-1.1. Baseline Project: The Strömgren Spheres of Quasars During the EOR

Proposal AG686 covers a first installment of observing time for the baseline project discussed in this Appendix. This will enable investigation of the hypothesized strong signal case of Wyithe & Loeb (cold IGM) and first demonstration of high sensitivity, high dynamic range imaging. Additional time will be requested in a subsequent VLA "large" proposal for follow-up and investigation of the hyptothesized weak signal case. AG686 has been nominally accepted for D configuration in 2005, pending technical and management review.

We consider observing the three known quasars believed to lie within the EOR ($z = 6.2 - 6.4$) for 250 hours each, with the VLA in D configuration. We adopt a 12.5 MHz total bandwidth with two polarizations and 16 spectral channels (after hanning smoothing) of 0.8 MHz width (1260 $\mathrm{km\,s^{-1}}$ or a physical line-of-sight scale due to the Hubble expansion of ~ 1.6 Mpc).[1] The expected rms per channel is 14 mK for a naturally weighted image (ie. optimal point source sensitivity), with a resolution of 7.″5 (2.5 Mpc). The diameters of the Strömgren spheres could be somewhat larger, depending on quasar age and assumptions of the cosmological model. (u,v)-tapers will probably be used to match the beam to the source size (see below).

Good spectral coverage is crucial for subtracting the foreground continuum emission (radio galaxies and the Galaxy), and we will explore a number of techniques for dealing with this continuum emission. First, we will obtain a short (12 hour) integration in the A array to find the brighter point sources in the field ($\geq$ 10mJy). These will be subtracted from the UV data. We will then fit baselines (simple power-laws or slowly curving functions) to the spectral data to remove the Galactic emission, and residual radio galaxy emission. Clearly, continuum subtraction will be one of the more challenging aspects of the experiment, since the foregrounds have to be removed to the level of a few$\times 10^4$. We will experiment with real and simulated data using both image-plane and uv-plane subtraction, as well as with the three-dimension fourier analysis techniques proposed in, e.g., Morales & Hewitt (2004).

The magnitude of the signal for a cosmological Strömgren sphere (CSS) depends on whether the spin temperature of the IGM is above or below the CMB temperature. For the "warm IGM" case, we have used the program UVCON in AIPS to simulate a data set for a quasar, using the models in Wyithe & Loeb (2004a) with a neutral fraction of $f(HI) = 1$

[1]The number of channels and bandwidth are limited by the current VLA correlator. While these are adequate for the current experiment, the future EVLA correlator will allow for many more channels over a wider bandwidth. One ramification will be improved RFI excision.

(their Figure 4, upper panel). This model implies a brightness temperature ~ 20 mK and a radius on the order of 5-15$'$, depending on quasar age and isotropy of ionization. (For the "cold IGM" case, the signal is ~ 15 times larger.)

Figure 10 shows simulated images. The left panel shows a full resolution image (7$'$.5), while the right panel shows a tapered image with a resolution of 15$'$, both for one spectral channel. Because the (u,v)-coverage of the VLA is centrally concentrated, such that the rms increases only slowly as the taper increases, until one reaches the central "hole," which for the VLA D configuration starts at ~ 75 m. Hence, the rms on the full resolution image is 0.09 mJy, while that on the tapered image it is 0.12 mJy. These correspond to brightness temperature sensitivities of $\sim$ 16 mK and 5.3 mK, respectively. The signal is expected in two channels (improving the RMS by $\sqrt{2}$), and its position on the sky is known. The combination of spectral and spatial information will be critical for verification of the line signal, these simulated images show that even for the weak signal case (a warm IGM) we will be able to test models effectively, e.g., constrain angular size and rule-out a universe for which $f(HI) > 0.5$ at $z \sim 6.2$. This will set the first hard limits on the cosmic neutral fraction at the end of cosmic reionization.

We emphasize that, while analyses of the Gunn-Peterson effect and the WMAP large scale polarization results have constrained the EOR to be between $z = 6$ and 17, current data provide only crude lower limits to the neutral fraction at $z \sim 6.3$ of 10^{-3}. Arguments have been made for high neutral fractions, > 0.1 (Wyithe & Loeb 2004a), and for low neutral fractions, < 0.01 (Oh & Furlanetto), based on optical spectra of $z \sim 6$ quasars. It is unlikely that further analyses of line of sight absorption information provided by optical spectra will constrain the neutral fraction and better than has been done so far. In contrast, the direct detection of line emission from HI and imaging of its distribution on the sky is a more simple approach and one that appears more likely to provide hard limits.

B-1.2. General Advantages of a VLA/EVLA VHF System for EOR Studies

For a very modest investment, the VLA will be competitive with and complementary to other near-term experiments intended to detect HI during the EOR, such as PAST. Indeed, one could argue that having two or more complementary experiments is crucial when considering the scientific importantance of these programs, and the potential systematic problems that could dominate the errors.

Critical aspects of the VLA-VHF system relative to the other proposed experiments are the low cost and short timeline. The low cost is due to the highly leveraged aspect of the

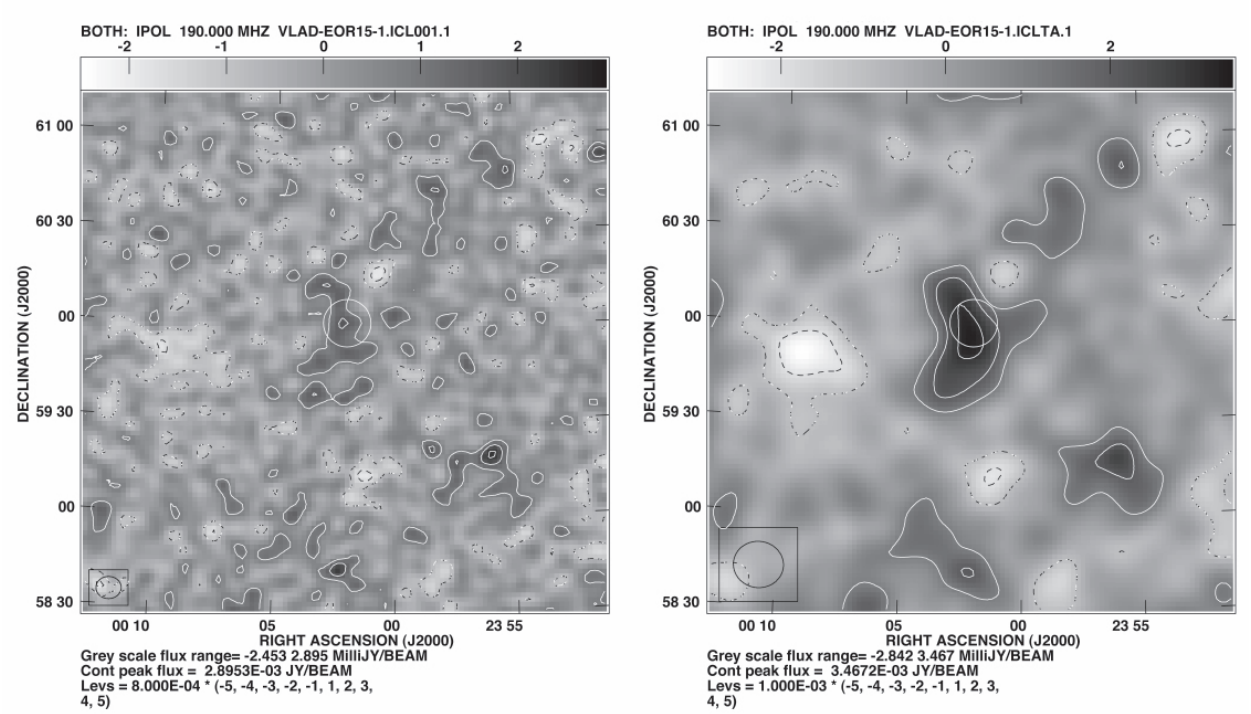

Fig. 10.— Simulation of VLA/EVLA observations of the HI signal from a CSS around a quasar at $z = 6.2$, assuming 250 hrs on source and a 0.8 MHz spectral channel separation. The central figure shows the naturally weighted image (7.″5 resolution, 0.09 mJy rms). The right image shows a tapered image (15′ resolution, 0.12 mJy rms). The circle shows the size of the sphere. The contour levels are linear, starting at 0.18 mJy beam^{-1} in the left figure, and 0.22 mJy beam^{-1}.

program, i.e., we already have telescopes, and IF and correlator system. All we need are receivers. And fortuitously, the VLA/EVLA u,v-coverage, and primary beam, are reasonably well matched to what is required. The time-line can be agressive for the same reasons, as well as the relative simplicity of the required VHF receivers.

Another advantage enjoyed by the proposed VLA-VHF system is operation at the higher end of the frequency range where potential EOR signals can be detected. Consequently, problems related to the ionosphere and wide field imaging are mitigated. Experience at the GMRT at 230 MHz shows that the ionosphere is often reasonably well behaved, even on baselines out to 10 km, such that normal phase and amplitude calibration procedures can be employed. In particular, the $\sim 4^\circ$ FOV of the VLA/EVLA is comparable to the isoplanatic patch for ionospheric phase fluctuations, such that existing single-solution self-calibration techniques can be employed.

Of course, the disadvantage could be that the neutral fraction toward the end of the EOR ($z \sim 6.2$) may be low ($f(HI) \leq 0.1$), but testing this possibility is exactly what drives the proposed program. Indeed, the EOR programs have been designed such that even non-detections lead to ground-breaking, fundamental conclusions concerning the process of cosmic reionization.

B-1.3. Legacy Science Programs

The VLA-VHF system has been proposed and funded based on the desire to investigate CSSs. However, the system will given to the NRAO for general use by the VLA/EVLA community. In general, the addition of an observing waveband below the existing 320 MHz band will enable broadening of radio source spectral index studies to a regime in which phenomena such as low-energy cutoffs may be important. In this section we consider some of the other high profile science that could be performed with the VHF system. Rather than present a "laundry list" of potential science programs, we consider only a few potential ones, based on general observing capabilities. The science cases developed for LOFAR and the MWA (http://www.lofar.org, http://web.haystack.mit.edu/MWA/) include more complete compilations.

B-1.3.1. Wide-field Surveys

Since imaging noise decreases as the square root of integration time, a figure of merit for wide field surveys is (beam area)/(system noise)^2. To compare surveys at different frequencies, we also need to correct the noise rms to a fiducial frequency assuming a typical source spectral index. We assume a power-law of index -1 ($S_\nu \propto \nu^\alpha$) and use 74 MHz as the fiducial frequency. Column 11 in Table 1 shows a scaled "survey speed" for the VLA bands with the largest fields of view. The combination of large field, relatively low system noise, and low observing frequency, make the proposed VHF system the optimum frequency for surveys of the dominant population of cosmic radio sources.

Wide field low-frequency surveys will reveal high-redshift radio galaxies, giant radio galaxies, radio halo and relic sources (see http://www.lofar.org). For instance, in ~ 100 h a 190 MHz system could cover of order 10^4 deg^2 to 2 mJy rms, or a factor 3 deeper than the WENSS survey at 327 MHz (assuming $\alpha = -1$). For such a survey we expect about 6×10^5 sources. Below a few mJy it is well known that the source populations should change from mostly radio loud AGN to star forming galaxies. About half of the detected sample would

be star forming galaxies at $z \leq 1$.

B-1.3.2. Power Spectrum of HI Brightness Fluctuations at the EOR

In addition to the baseline CSS experiment, a second EOR-related experiment would be a study of the power spectrum of HI brightness temperature fluctuations over the full $\sim 4^\circ$ FOV due to the evolution of density and ionization in the IGM (Zaldarriaga, Furlanetto, & Loeb 2004). It is important to realize that the VLA/EVLA will not have the sensitivity to image the fluctuations. But an interferometer is a natural "Fourier filter," and the data can be averaged in the (u,v)-plane to obtain a power spectrum of density fluctuations. One gains a factor $\sqrt{2}$ in SNR due to the fact that the visibility phases are not relevant in such a statistical (i.e., power-spectrum) analysis. Adopting reasonable assumptions about symmetry enables a dramatic improvement in the detectability, in a statistical sense, of the fluctuations on a given scale. The situation is analogous to COBE and WMAP studies of fluctuations in the CMB, with COBE determining the statistics of the signal, and WMAP making a real image of the fluctuations (White et al. 1998).

Figure 11 shows the predicted angular power spectrum for $z = 7$ due to the evolution of the neutral IGM (Zaldarriaga et al. 2004). The error bars represent the VLA 1σ errors after 250 hours on source. For a ionization fraction of 0.75, we obtain a 3 to 5 σ detection of the power spectrum of the fluctuations in at least two (u,v)-annuli per 0.8 MHz spectral channel. There are 15 channels, and an optimal filtering can be performed to best match the size scale of the fluctuations to their frequency structure.

The most relevant experiment for comparison to the proposed program is the PAST experiment, since both are "path finders" with timescales of just a couple of years. Other experiments (e.g., LOFAR, MWA) have significantly longer timescales and much larger costs (> 4 years, $\gtrsim \$10^7$). The PAST experiment is being designed to have relatively uniform (u,v)-coverage out to baselines of a few to perhaps 10 km, leading to both good sensitivity on small angular scales ($l \geq 1000$, or $\theta \leq 0.2^\circ$) and relatively flat sensitivity as a function of scale. The VLA observations will complement PAST by enabling study of larger scale fluctuations ($\theta = 0.1^\circ$ to 0.3°). The centrally condensed (u,v)-coverage of the VLA, and the limited range of angular scale lead to a narrow peak in sensitivity for the power spectral analysis. Fortunately, this regime corresponds closely to an interesting range in the expected fluctuations.

B-1.3.3. HI Absorption Toward Radio Loud Sources During the EOR

A third EOR HI experminent is a search for absorption by the neutral IGM toward the radio loud AGN that existed during the EOR. This work could be performed with a VHF system and the EVLA correlator. Carilli, Gnedin, & Owen (2002) predict the expected absorption signal due to the neutral IGM during the EOR. Two signals are present: a "21 cm forest" of narrow lines (few $\mathrm{km\,s^{-1}}$) due to filamentary structure in the "cosmic web," (analogous to the Lyα forest seen after reionization) and an overall depression in the continuum due to the mean neutral IGM (analogous to the Gunn-Peterson effect). The proposed VHF system will be able to detect the line forest for a sufficiently bright radio source (probably $\sim$ 1 Jy). There is also the possibility of detecting stronger lines toward fainter radio sources by gas in the host galaxies of the radio sources, including (possible) prompt radio emission from GRBs and GRB afterglows (Furlanetto & Loeb 2003).

Figure 12 shows a simulated spectrum with the VLA for 250 hours toward a bright (1 Jy) radio source within a still largely neutral IGM. We expect about one absorption line per 0.5 MHz bandwidth with optical depth $\geq 1\%$ due to the 21 cm forest. These would be detected at the EVLA at $\geq 5\sigma$. If we include possible absorption by "mini-halos," the line density would increase by a factor two. Obviously, the absorption experiment rests on the discovery of the first radio loud AGN inside the observing band of the proposed VHF receivers ($z = 6.2$-6.9). Current models (Rawlings & Jarvis 2004), predict that there should be at least a few (of order 10) radio sources brighter than 1 Jy at $z > 6$ over the sky. Indeed, candidates sources have already been found (de Breuck 2000; Rawlings and Jarvis 2004).

B-1.3.4. The Transient Universe: Prompt (Coherent) Emission from GRBs

Gamma-ray bursts (GRB) represent physics at its most extreme, with large energy releases (10^{51} erg), ultra-relativistic shocks ($\Gamma_\circ \sim$100), and large magnetic fields ($\sim$100 G). If an average GRB were to release only a tiny fraction of its energy (10^{-6}) into the radio band, then it would produce emission bright enough ($\sim$100 Jy) to be detected by existing instruments. Prompt, coherent emission has also been predicted by several recent theoretical studies (e.g. Sagiv & Waxman 2002). However, quantitative flux estimates are difficult to obtain by this approach because we lack any real physical understanding of the detailed plasma properties of GRB outflows (i.e., baryonic versus Poyntying flux).

Ginzburg (1973) was the first to anticipate the rich scientific rewards that the detection of prompt radio emission from a GRB would bring. An electromagnetic signal of frequency ν traveling through an ionized medium will experience a dispersive delay $\Delta t \propto \mathrm{DM}/\nu^2$, where

the dispersion measure (DM) is the integrated free electron density along the line of sight DM=$\int n_e dl$. The dispersion measure has at least four components: (*i*) our Galaxy, (*ii*) the intergalactic medium (IGM), (*iii*) the GRB host galaxy, and (*iv*) the circumburst medium. Depending on the expected ionized column density towards GRBs, it is possible, with a sufficiently fast telescope, to slew to the location of a burst and begin observing *prior* to the arrival of the radio signal. A successful detection will not only shed light on GRB central engine properties, but it would provide a powerful new probe of the circumburst environments of GRBs, allow us to search for the missing baryons at moderate z, and probe the epoch of reionization at high z (Palmer 1993, Ioka 2003, Inoue 2004).

In Figure 13 we show the delay times at low frequencies for a range of column densities (or DM). Detailed simulations have been carried out for a population of GRBs as part of VLA project AF 419 to estimate the total DM. The ionized column density is found to range from few$\times 10^{21}$ to 10^{23} cm^{-2}, corresponding to 1000<DM<30,000 cm^{-3} pc. These estimates are in line with observational constraints from measurements of the GRB gas columns estimated from optical extinction, X-ray photoelectric absorption and damped Lyα absorbers (Stratta et al. 2004; Vreeswijk et al. 2004). The largest uncertainty comes from our rather sketchy understanding of the circumburst environment and the extent to which GRBs might photoinize it (Perna & Lazzati 2002).

A successful experiment must be able to slew the VLA/EVLA to the burst position within a time that depends on the observing frequency and the DM. The VLA/EVLA antennas can slew to any location on the sky within 9 minutes (the distribution of slew times peak at 2.5 minutes). At 74 MHz this requirement is easily met, but beyond 10^{22} cm^{-2} the time delay over which the search is conducted becomes unreasonably large ($>$ 1 hr). This limitation can be offset by simultaneously searching at 327 MHz, a frequency that is sensitive to high DMs. This dual 74/327 MHz approach is what is currently planned for AF 419.

Alternatively, we can use an intermediate frequency. The 190 MHz band clearly is an ideal frequency in which to conduct a sensitive search for prompt, coherent radio emission from a GRB. For the range of DMs above, we expect time delays of approximately 4 to 60 minutes after a burst. This allows the VLA/EVLA to be be on source prior to the arrival of the signal. Our simulations indicate that by using burst alerts provided by the *Swift* satellite, the VLA/EVLA will be on source prior to the arrival of the putative signal 75% to 100% of the time. Furthermore, the superior sensitivity and cleaner interference environment expected at 190 MHz will aid in the detection of a signal in the time domain. Confirmation of any candidates (by imaging the visibilities) will likewise be simplier at 190 MHz than at 74 MHz.

B-1.3.5. Radio Recombination Lines

Hydrogen Radio Recombination Lines (RRL) arise close to ionizing sources, located typically in relatively dense regions. In contrast, Carbon RRLs arise in the surface layers of dense regions and in the diffuse ISM. The ionization potential for neutral Carbon is slightly below that for Hydrogen. As a result, radiation slightly too weak to ionize Hydrogren escapes into the ISM where it can be responsible for RRL emission and absorption features from Carbon in the surrounding material. The passband of the proposed VHF system includes transitions close to $\sim$C(320α). The combination of VHF and 320 MHz maps of RRL emission/absorption may be used to constrain conditions in the ISM better than 320 MHz alone because the transitions are widely separated and the specific intensity of background emission will differ substantially between wavebands. We also note that the detection of the effects of dielectronic recombination may also be possible (Walmsley & Watson 1982), enabling broader studies of relative line intensities.

B-1.3.6. Pulsars

A VHF observing system would achieve high sensitivity at frequencies where pulsar emission is strong because of steep spectral indices. The proposed system would especially benefit millisecond pulars surveys of globular clusters, for which dispersion measure is small and spectra steeper than the median. A comparison of sensitivities for the VLA/EVLA and single dish facilities operating at higher frequency (e.g., the Lovell telescope, Effelsberg) is difficult in advance of VHF field testing, but it is reasonable to expect VLA/EVLA studies to be competitive. In principle, searches for giant pulses in long integrations may be feasible because of the large primary beam of the VLA/EVLA at VHF frequencies and the very steep spectrum of these particular pulses.

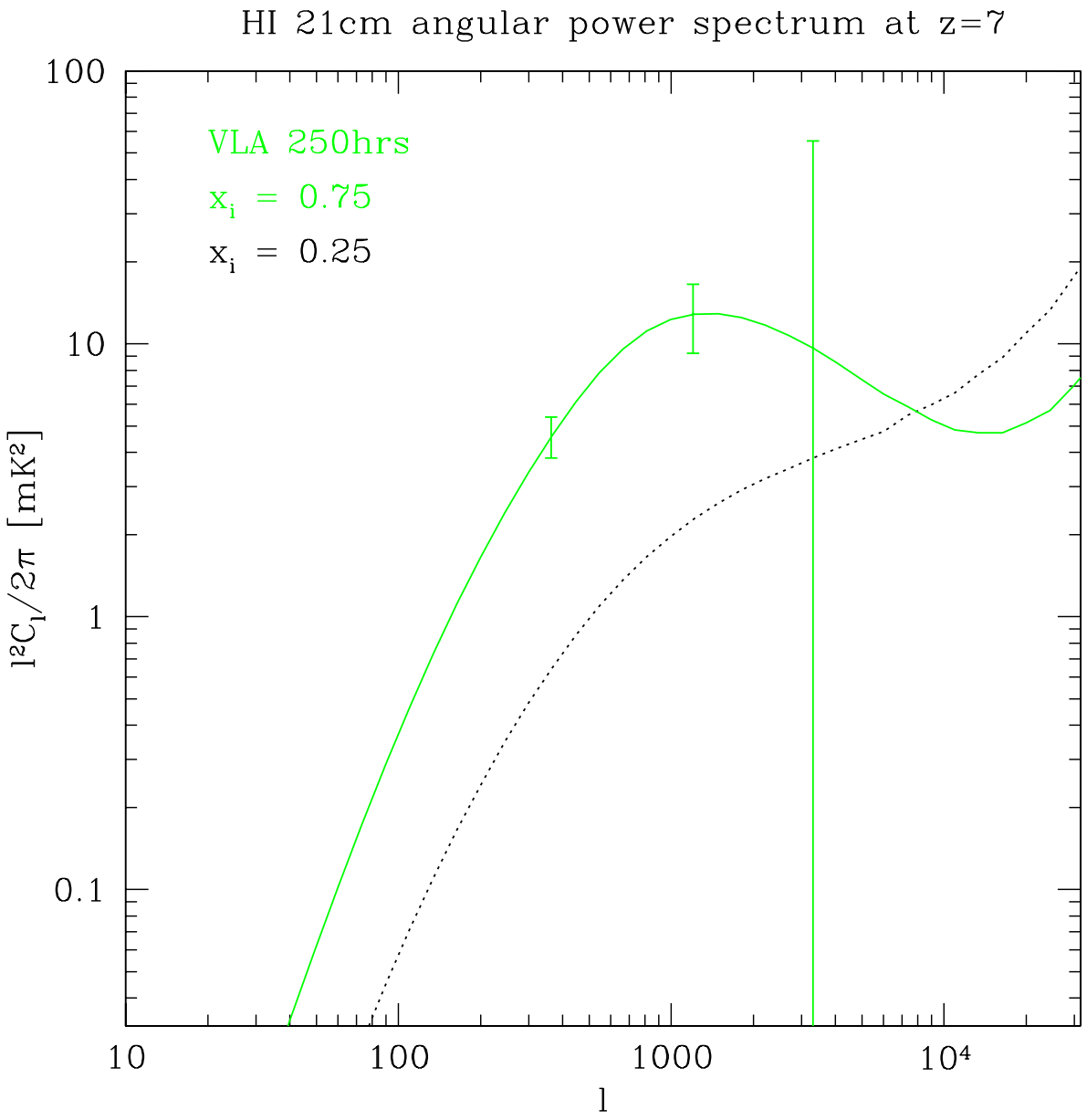

Fig. 11.— The angular power spectrum of HI brightness fluctuations at $z = 7$, plus VLA/EVLA measurement errors in a 0.8 MHz spectral channel averaged over three annuli in (u,v)-space. The solid line shows the expected signal for an ionization fraction of 0.75, while the dotted line shows an ionization fraction of 0.25.

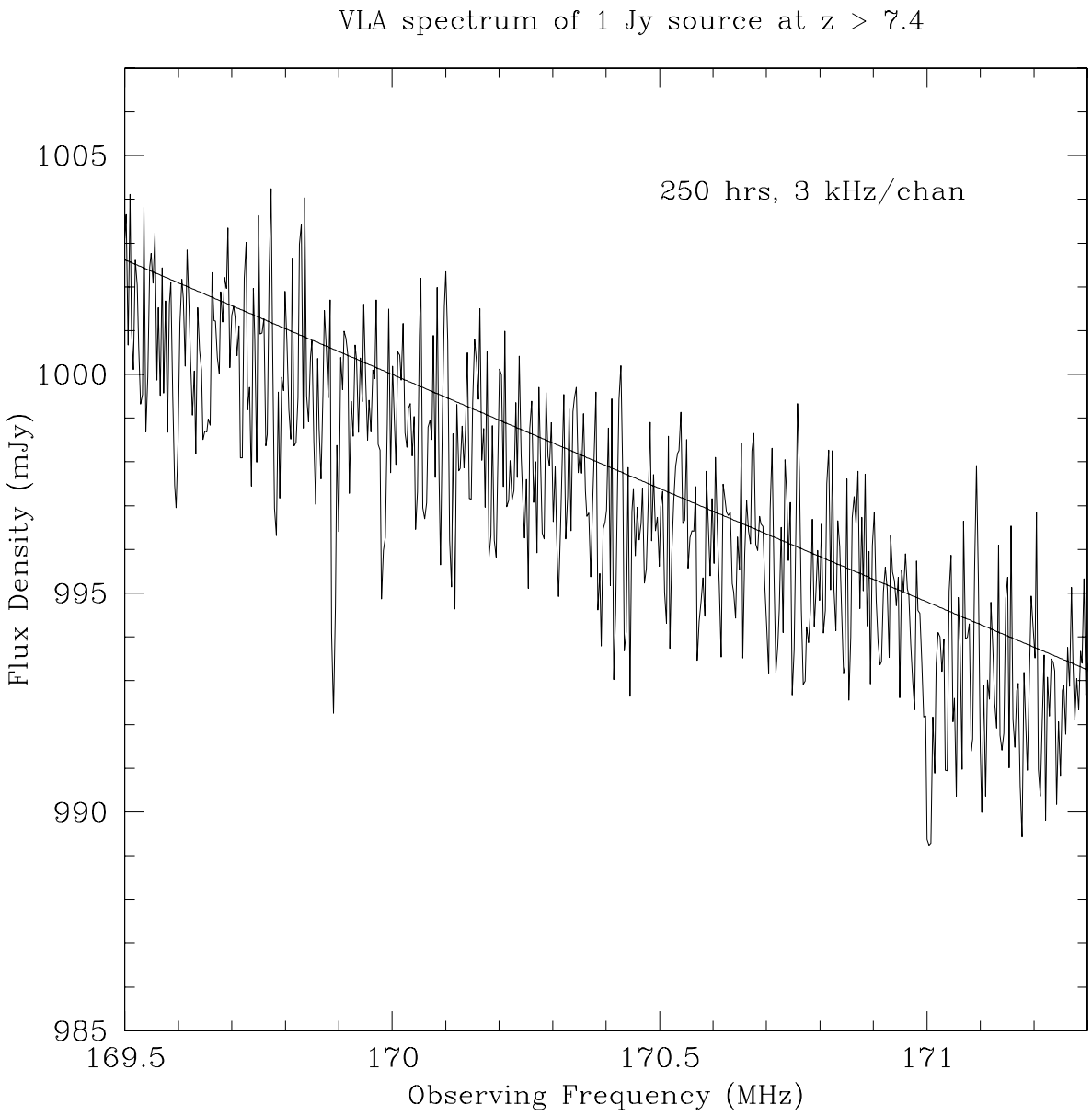

Fig. 12.— A simulated HI absorption spectrum of a $z > 7.4$ radio loud AGN. The solid line is the power-law continuum.

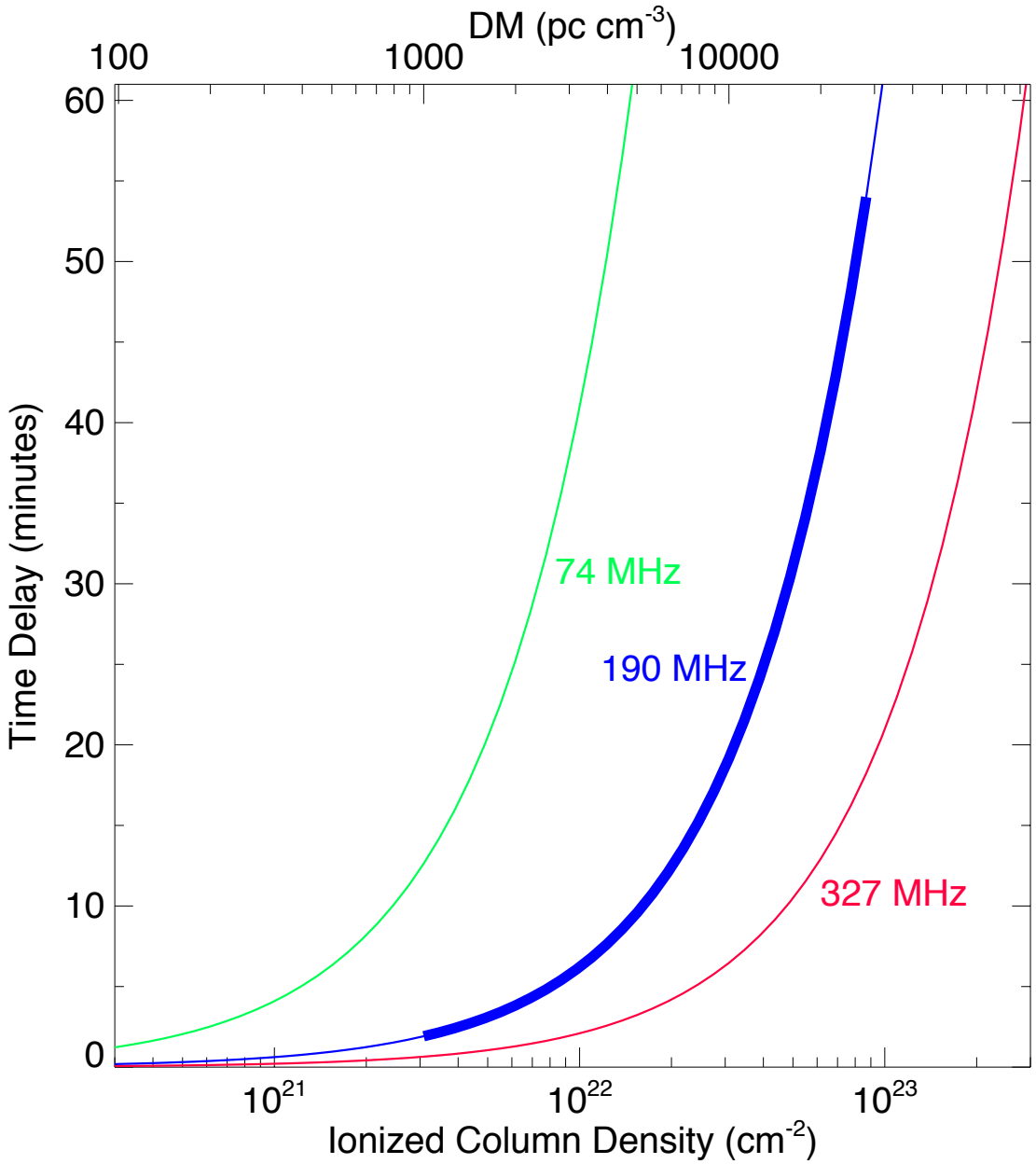

Fig. 13.— The delay in the arrival times of signals which are propagating through ionized gas as a function of the column density (or equivalently the dispersion measure, DM). The delay is a function of frequency so the two existing VLA low frequency bands are plotted, as well as the proposed 190 MHz band. Given the expected range in the ionized column density towards GRBs (thick blue line), the choice of 190 MHz is an ideal frequency for this VLA experiment (see text for more details).